

Laser-evoked synaptic transmission in cultured hippocampal neurons expressing channelrhodopsin-2 delivered by adeno-associated virus

Jennifer Wang^{a,*}, Mazahir T. Hasan^b, H. Sebastian Seung^c

^a Department of Brain and Cognitive Sciences, Massachusetts Institute of Technology, 77 Massachusetts Avenue 46-5065, Cambridge, MA 02139 United States

^b Max Planck Institute for Medical Research, 29-Jahnstrasse, D-69120 Heidelberg, Germany

^c Departments of Brain and Cognitive Sciences and Physics, Massachusetts Institute of Technology, Howard Hughes Medical Institute, 77 Massachusetts Avenue 46-5065, Cambridge, MA 02139, United States

ARTICLE INFO

Article history:

Received 1 April 2009

Received in revised form 17 June 2009

Accepted 18 June 2009

Keywords:

Channelrhodopsin-2 (ChR2)

Recombinant adeno-associated virus (rAAV)

Synaptic physiology

Primary hippocampal culture

ABSTRACT

We present a method for studying synaptic transmission in mass cultures of dissociated hippocampal neurons based on patch clamp recording combined with laser stimulation of neurons expressing channelrhodopsin-2 (ChR2). Our goal was to use the high spatial resolution of laser illumination to come as close as possible to the ideal of identifying monosynaptically coupled pairs of neurons, which is conventionally done using microisland rather than mass cultures. Using recombinant adeno-associated virus (rAAV) to deliver the ChR2 gene, we focused on the time period between 14 and 20 days *in vitro*, during which expression levels are high, and spontaneous bursting activity has not yet started. Stimulation by wide-field illumination is sufficient to make the majority of ChR2-expressing neurons spike. Stimulation with a laser spot at least 10 μm in diameter also produces action potentials, but in a reduced fraction of neurons. We studied synaptic transmission by voltage-clamping a neuron with low expression of ChR2 and scanning a 40 μm laser spot at surrounding locations. Responses were observed to stimulation at a subset of locations in the culture, indicating spatial localization of stimulation. Pharmacological means were used to identify responses that were synaptic. Many responses were of smaller amplitude than those typically found in microisland cultures. We were unable to find an entirely reliable criterion for distinguishing between monosynaptic and polysynaptic responses. However, we propose that postsynaptic currents with small amplitudes, simple shapes, and latencies not much greater than 8 ms are reasonable candidates for monosynaptic interactions.

© 2009 Elsevier B.V. All rights reserved.

1. Introduction

The cloning of channelrhodopsin-2 (ChR2) and subsequent expression in mammalian cells promised to revolutionize neurophysiology because it enabled optical stimulation of neurons in a spatially localized and temporally precise fashion (Boyden et al., 2005; Nagel et al., 2003; Wang et al., 2007). ChR2 has been used to identify presynaptic partners of an electrophysiologically recorded postsynaptic neuron (Arenkiel et al., 2007; Petreanu et al., 2007; Wang et al., 2007). Other applications include mapping neuronal circuits, probing synaptic function in genetically defined populations of neurons, and inducing plasticity at single synapses (Atasoy et al., 2008; Liewald et al., 2008; Wang et al., 2007; Zhang et al., 2008; Zhang and Oertner, 2007). In principle, ChR2 could also be used to study the responses of networks to complex spatiotemporal patterns of stimulation.

Expression of ChR2 in neurons has been achieved by mouse transgenesis (Arenkiel et al., 2007; Wang et al., 2007); *in utero* electroporation (Petreanu et al., 2007), lentivirus (Boyden et al., 2005) and recombinant adeno-associated virus (rAAV) (Bi et al., 2006). A major drawback of lentivirus is that its DNA integrates into the host genome. Therefore the transgene is potentially susceptible to integration-induced epigenetic silencing (Ellis, 2005; Xia et al., 2007). Furthermore, a host gene could be disrupted by lentivirus DNA integration, which could affect normal neuronal function. Although mouse transgenesis by oocyte DNA injection is a powerful tool, integration of exogenous DNA at specific sites can lead to integration-induced gene silencing (Clark et al., 1997; Robertson et al., 1996) and position-effect variegation (Robertson et al., 1995) with gene expression in some cells but not others. Although a plasmid delivered by *in utero* electroporation remains extrachromosomal, which may alleviate the silencing problem, transfection of early progenitor cells leads to mosaic gene expression in neuronal populations of the postnatal brain (Borrell et al., 2005; Hatanaka et al., 2004).

Recombinant adeno-associated virus gene delivery has been successfully used to express ChR2 in mouse retinal neurons, and

* Corresponding author. Tel.: +1 617 452 2691; fax: +1 617 452 2913.

E-mail address: jenwang@mit.edu (J. Wang).

expression was reported to be stable for a year (Bi et al., 2006). We chose rAAV for introducing ChR2 in cultured hippocampal neurons for several reasons. First and foremost, genetic modules introduced into rAAV are less prone to epigenetic gene silencing. Second, long-term expression, from months to years, is achievable. Due to high rate of infectivity, rAAV can be used to introduce multiple genes into the same neurons in pre-selected brain regions (Shevtsova et al., 2005) without epigenetic silencing (Zhu et al., 2007). This broadens the experimental possibilities so that other genes whose products act as biosensors for different signaling systems, such as for calcium (Miyawaki, 2003; Palmer and Tsien, 2006; Wallace et al., 2008) and neurotransmitter release (Miesenböck et al., 1998), could also be introduced into the same neuron using rAAV as the delivery method. This would make it possible to optically record functional neuronal connectivity without the need to use patch pipettes. Moreover, by gene selective knockdown of endogenous protein levels using small interfering RNA (siRNA) (Fountaine et al., 2005), especially under control of the tetracycline-controlled systems (Hasan et al., 2004; Sprengel and Hasan, 2007), it should be possible to correlate how changes in gene activity affect neuronal circuits and animal behavior (Grillner, 2006; Kandel, 2001).

Additionally, the rAAV gene delivery method allows targeting of selective brain regions, which makes it especially powerful for *in vivo* applications. ChR2 has also been targeted to genetically defined populations of neurons through cell-type specific promoters and Cre-dependent constructs to examine neural circuits based on cell types (Atasoy et al., 2008; Liewald et al., 2008). Availability of different AAV serotypes provides additional means to selectively target different neuron types (Burger et al., 2004; Shevtsova et al., 2005; Tenenbaum et al., 2004).

Another feature of rAAV is that it shows low immunogenicity over a long time span (Sun et al., 2002), a key safety criterion that has made rAAV gene delivery the method of choice for therapeutic treatment of animal diseases, including humans. Therefore, rAAV-mediated delivery of ChR2 should not only help to investigate functional brain circuits in living animals but it may also provide a plausible approach to treat neurological diseases which require deep brain stimulation (Gradinaru et al., 2007; Mehrkens et al., 2008; Obeso et al., 1997).

The preceding considerations are general reasons for using rAAV to introduce the ChR2 gene into neurons. Our goal in this paper was to develop the ChR2 method specifically for studying evoked synaptic transmission in mass cultures of dissociated hippocampal neurons.

Dual intracellular recording from pairs of dissociated hippocampal or neocortical neurons is a widely accepted method of studying synaptic plasticity (Arancio et al., 1995; Bi and Poo, 1998; Goda and Stevens, 1996; Kaplan et al., 2003). Such experiments are often done with low density cultures. In one culture method, the substrate that the neurons grow on is sprayed in a mist onto the coverslips, making dots that are less than 1 mm in diameter. Then neurons are plated at low density. The microdots physically limit the neurons' growth so that some microislands end up with just a few neurons or even just two (Bekkers and Stevens, 1991, 1995; Segal and Furshpan, 1990). Within such a microisland, the probability of connection is high, so that it is straightforward to find connected pairs of neurons (Kaplan et al., 2003). In another culture method, neurons and glia are plated at the same time at low density, and this also leads to growth of isolated pairs of neurons (Wilcox et al., 1994).

While the microisland technique makes it easier to record from pairs, culturing healthy neurons becomes more challenging at lower densities. Furthermore, pairs of neurons on microislands tend to be strongly coupled, probably by multiple synaptic contacts (Segal and Furshpan, 1990). Evoked postsynaptic currents are typically hundreds of picoamperes or more, while sponta-

neous postsynaptic currents ("mini"s) are tens of picoamperes or less (Wilcox et al., 1994). A low calcium solution combined with microperfusion of a high calcium, hypertonic solution (Bekkers and Stevens, 1995) has been used to reduce the amplitude of evoked postsynaptic currents by permitting activation of only a small subset of synapses between two neurons. But without this kind of manipulation, postsynaptic currents evoked in microisland cultures are much larger than those recorded in brain slice experiments.

For these reasons, we have been interested in using mass cultures for synaptic plasticity experiments. These types of cultures are relatively easy to grow and keep healthy, because neurons can be cultured at higher densities. But in our experience, it is difficult to find connected pairs by intracellular recording of randomly chosen neurons, because the probability of connection is low. ChR2 could potentially solve this problem, by allowing the screening of many candidate neurons to find presynaptic partners of a single postsynaptic neuron. We could do this by expressing ChR2 in the culture, and then stimulating presynaptic neurons with a laser while patch recording from a single neuron. If a stimulated neuron is monosynaptically or polysynaptically connected to the recorded neuron, a synaptic response should be observed.

For this purpose, we needed a delivery method for ChR2 that reliably resulted in viable cells, adequate expression levels, and expression during the right time window. We also needed a method of optical stimulation that was spatially precise and reliably evoked action potentials.

In dissociated cultured neurons, experiments on synaptic physiology are typically done between one and three weeks *in vitro* (Arancio et al., 1995; Bekkers et al., 1990; Bekkers and Stevens, 1995; Bi and Poo, 1998; Goda and Stevens, 1996; Gomperts et al., 2000; Kaplan et al., 2003). Earlier than one week, there is little or no synaptic transmission (Gomperts et al., 2000). After three weeks, there is typically spontaneous synchronous bursting (Pasquale et al., 2008; van Pelt et al., 2004a,b), which could interfere with plasticity experiments. For this reason, we were interested in characterizing the expression of ChR2 during this time window. Based on the fluorescence of a ChR2-YFP fusion protein, expression starts at about one week, and is strong after about two weeks *in vitro*. Infected cells looked as healthy as uninfected cells, as they could not be distinguished from each other in phase contrast images.

To characterize the effectiveness of optical stimulation, we performed patch clamp recordings of neurons while simultaneously illuminating them transiently. After two weeks *in vitro*, about 80% of infected cells could be stimulated to generate action potentials using wide-field illumination. Stimulation by laser was more difficult, and depended on the size of the illuminated spot. A 40 μm diameter spot stimulated approximately one third of infected neurons, whereas a 10 μm diameter spot stimulated only one quarter. This demonstrated a trade-off between the fraction of cells that can be stimulated, and the accuracy of spatial localization of stimulation. The luminance of the spot had little effect, if it was above a threshold value. If a cell could be stimulated to fire an action potential, then this response was highly reliable every time it was illuminated.

Our next goal was to investigate the best means of using ChR2 to study synaptic transmission. We performed patch clamp recordings of neurons that were not expressing ChR2, or only weakly, in order to reduce the possibility or magnitude of direct stimulation by light. Then we scanned the laser across multiple locations arranged in a grid. Many types of responses were recorded in the patch clamped neuron, which appeared to be direct, monosynaptic, or polysynaptic. Based on classification of these responses, we propose a criterion for identifying possible monosynaptic pairs of neurons using amplitude, shape, and latency of the recorded currents.

2. Materials and methods

2.1. Preparation of rAAV

The viral expression construct rAAV-P_{hSYN}-Chr2-YFP was constructed by subcloning the Chr2-YFP fragment (Boyden et al., 2005) into an adeno-associated (serotype-2) viral expression cassette with the human synapsin promoter (P_{hSYN}), a woodchuck post-transcriptional regulatory element (WPRE), and a bovine growth hormone (BGH) polyadenylation sequence (Shevtsova et al., 2005). rAAV was prepared by transfecting HEK293 cells with the plasmid rAAV-P_{hSYN}-Chr2-YFP together with helper plasmids (Grimm et al., 2003), pDp1 (serotype 1) and pDp2 (serotype 2) in a ratio of 3:1 harboring expression cassettes for replicase and capsid proteins. Seventy-two hours after transfection, HEK293 cells were washed once with phosphate-buffered saline (PBS) and collected into 50 ml falcon tubes, pelleted by centrifugation and resuspended in lysis and digestion buffer supplemented with benzonase (Sigma) at 37 °C for 30 min and with NaCl at 50 °C for 30 min. Cell debris was removed by centrifugation at 6000 rpm and clear supernatant was frozen at –70 °C. For harvesting pure virus, the supernatant was thawed on ice and layered on an idoxanol (Progen, Germany) gradient (Auricchio et al., 2001). Centrifugation was done for 60 min, and the virus located on top of the 40% idoxanol layer was removed and placed into a 15 ml falcon tube. To remove salt and further concentrate the virus, the idoxanol gradient fraction was washed three times with PBS and concentrated to a volume of 200–300 μ l using Amicon filters (Amersham). Infectious virus titers were determined in primary neuron cultures as described previously (Zhu et al., 2007).

2.2. Primary dissociated cell culture

Dissociated primary cultures of rat hippocampal neurons were prepared in 24-well plates as described previously (Hagler and Goda, 2001). Hippocampi were extracted from P0 rat pups, rinsed three times in HBSS, incubated with an enzyme solution containing 1 mM L-cysteine, 0.5 mM EDTA, 1.5 mM CaCl₂, 200 units Papain (Worthington), and 0.1 μ g/ml DNase in a modified HBSS (contains an additional 25 mM HEPES, pH 7.3) for 30–40 min, and then mechanically triturated with a fire-polished pipette. The cells were counted on a hemocytometer and diluted in culture medium containing 6 mg/ml glucose, 1 mM Na-Pyruvate (Invitrogen), 10% fetal bovine serum (Hyclone), 0.1% Mito serum extender (Invitrogen), 2% B27 (Invitrogen), and 1 mM HEPES (pH 7.3) in Basal Medium Eagle (Invitrogen), so that the plating density was 50,000 cells/mL. The cells were plated on 12 mm German glass coverslips (Electron Microscopy Sciences), coated with a mixture of 5.5 mM acetic acid and 0.9 mg/ml rat tail collagen (BD Biosciences). After 2 days, 20 μ M Ara-C (Sigma) was added to prevent further growth of glia.

The virus (rAAV-P_{hSYN}-Chr2) was added either to the cell suspension just before plating or 1 day after plating by adding 1–3 μ l of solution containing the virus for each well. The culture medium was not changed after adding the virus.

2.3. Electrophysiology

The culture was visualized using an inverted microscope (Olympus IX-70) and a QICam CCD camera (Qimaging). Whole cell recordings of membrane potential and currents were obtained using a patch clamp amplifier (Axon Instruments). The bath solution contained (in mM): NaCl 145, KCl 3, HEPES 10, CaCl₂ 3, glucose 8, MgCl₂ 2, pH 7.30 as described previously (Bi and Poo, 1998). To prevent washout of the intracellular milieu, we used a perforated patch solution containing (in mM): potassium gluconate 136.5, KCl

17.5, NaCl 9, MgCl₂ 1, HEPES 10, EGTA 0.2, pH 7.20 as described previously (Bi and Poo, 1998) with 300 μ g/ml Amphotericin-B (Sigma). Data were sampled at 10 kHz and collected using the Matlab XPC target toolbox. Sutter micromanipulators were used to position the patch pipettes.

The holding current for current clamp recordings was set to the leak current, which was defined to be the current measured when the neuron was voltage clamped at –70 mV.

2.4. Optical stimulation

Wide-field stimulation of patch clamped neurons was performed with an unfiltered XCite lamp, attached to the epifluorescence illumination port on the microscope.

Timing and synchronization with the electrophysiology for both wide-field and laser stimulation were achieved by triggering a mechanical shutter (Uniblitz) placed between the light source and the microscope. However, the opening time of the shutter did not occur synchronously with the trigger. We measured the time for the shutters to open using a silicon photodiode (Thorlabs). The delay in opening of the wide-field shutter (Model VS35) from the trigger time was measured to be 3.4 ± 0.1 ms (mean \pm standard deviation for five measurements), and the delay for the laser shutter (Model VS25) was 3.3 ± 0.04 ms (mean \pm standard deviation for five measurements). The reported latencies for the electrophysiological signals were calculated by measuring the time between the point of interest and the shutter trigger signal and then subtracting the mean shutter delay time from this difference.

A guided laser stimulation system was designed using a 30 mW 488 nm solid state laser (Coherent). The laser output was coupled to a fiber optic (Point Source), beam diameter expanded to 3 mm, passed through neutral density filters, directed into galvos (Cambridge Technologies, model 6210H) to move the beam, and sent through a scan lens so that the spot was focused in the image plane of the microscope (Olympus IX-70). A schematic of the optical system is shown in Fig. 3A.

The intensity of the laser measured at the sample ranged from 10 μ W to 1 mW. We measured the diameter of the laser spot size by sandwiching a drop of fluorescein between two coverslips and taking an image of the fluorescent excitation produced by the laser spot. We plotted the intensity values across a line centered over the spot. From the resulting profile, we calculated the diameter of the spot as the full width at half maximum (FWHM) intensity. The luminance was calculated using the intensity measurement at the sample, divided by the area of the laser spot, calculated from the FWHM.

To accurately stimulate specific locations in the culture, a map of control voltages for the galvos and the corresponding laser spot location in the image was created at intervals of 100 pixels. Values were interpolated between these points. Custom software was written in Matlab to guide the laser spot to particular spatial locations and control the mechanical shutter.

3. Results

3.1. rAAV mediated delivery of Chr2-YFP into neurons

To monitor the expression levels of Chr2 in neurons, the Chr2 gene was fused to a yellow fluorescent indicator protein (YFP) (Boyden et al., 2005) and cloned into a rAAV expression plasmid with the human synapsin promoter (P_{hSYN}) (Shevtsova et al., 2005) driving Chr2-YFP expression (rAAV-P_{hSYN}-Chr2-YFP) (Fig. 1A). Virus with capsid proteins of the serotype 1 and 2 was prepared as described previously (Zhu et al., 2007). The culture

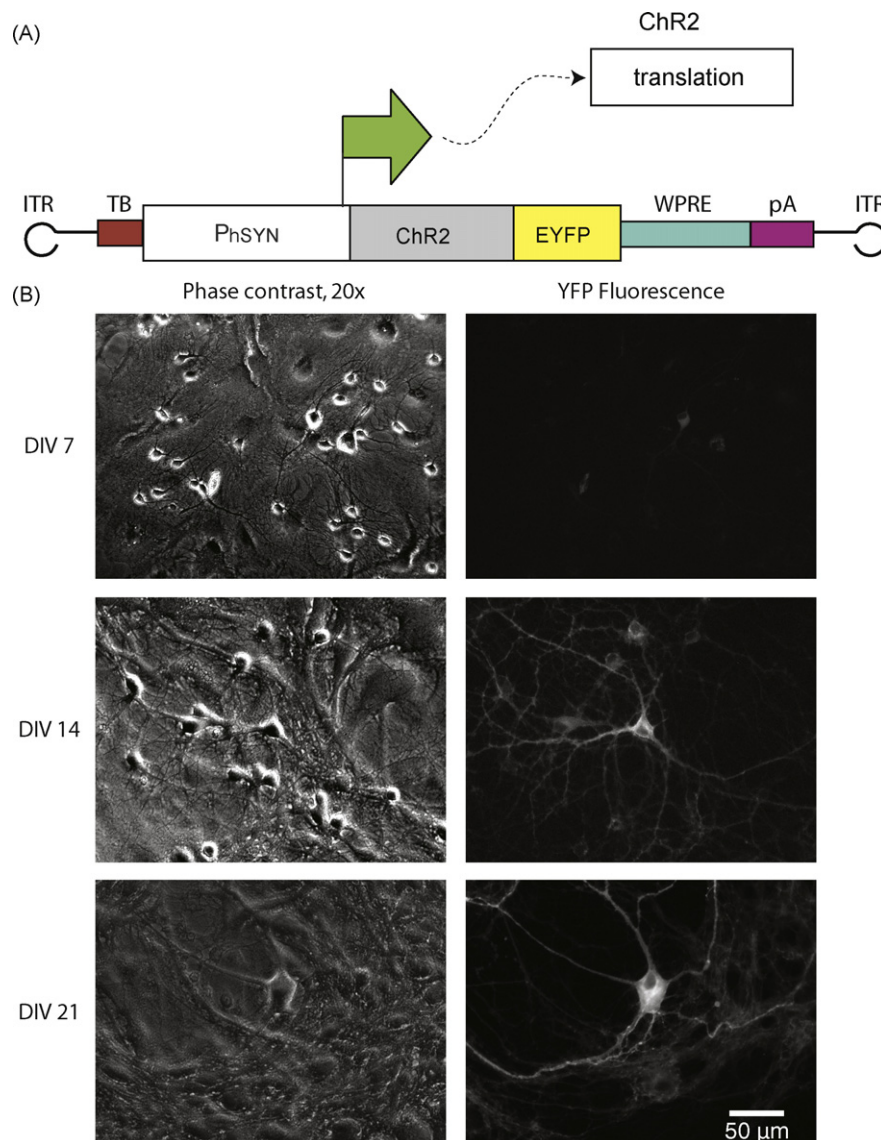


Fig. 1. (A) Expression cassette for rAAV-P_{hSYN}-ChR2. The human synapsin promoter (PhSYN) drives expression of ChR2-EYFP. Labels: synthetic transcription blocker (TB), a woodchuck hepatitis virus posttranscriptional control element (WPRE), polyadenylation signal (pA), inverted terminal repeats of AAV2 (ITR). (B) Left column shows phase contrast images of primary hippocampal culture at DIV 7, DIV 14, and DIV 21, magnified 20×. Right column has the same field of view as the left. The 50 μm scalebar applies to all images. Images were taken using an Excite lamp and YFP filter so that YFP fluorescence could be observed. Exposure time was fixed for all the fluorescence images so that visual comparison could be possible.

was infected with the virus, rAAV-P_{hSYN}-ChR2-YFP, 1–2 days after plating.¹ We observed YFP expression in the culture at 7, 14, and 21 days *in vitro* (DIV). Phase contrast and fluorescence images at 20× magnification are compared in Fig. 1B for these different time points. The exposure time is the same for all fluorescence images (2 s), so that image intensity should be directly proportional to YFP expression. Expression appears to begin around DIV 7, but does not reach high levels until DIV 14.

3.2. Wide-field stimulation of neurons expressing ChR2

We then assessed the effectiveness of wide-field stimulation as a function of days *in vitro*, spanning the time period from DIV 7 to DIV 27. Previous experiments performed on dissociated hippocampal

neurons were done between DIV 14 and DIV 28 and made no distinction between different time points in ChR2 expression (Boyden et al., 2005; Schoenenberger et al., 2008).

We performed current clamp recordings of neurons that were visibly expressing YFP (see Fig. 2A for diagram of experiment). We applied the synaptic blockers CNQX, APV, and bicuculline to ensure that responses were due to direct stimulation by light, rather than indirect stimulation through synaptic transmission. The neurons were stimulated with 5 pulses of broadband visible light for 10 ms per pulse. Sample traces from 3 neurons at DIV 7, 14, and 21 are shown in Fig. 2B.

Stimulation was defined as “reliable” if the neuron spiked in response to all 5 pulses of light. We quantified reliability as a function of days *in vitro* (Fig. 2D). The data were grouped so that week 1 included DIV 7 to DIV 13, week 2 included DIV 14 to DIV 20, and week 3 included DIV 21 to DIV 26. In week 1, only 29% of neurons showed reliable stimulation ($n=7$), consistent with the weak YFP signal reported above. This increased to 71% in week 2 ($n=14$) and

¹ Previous experiments in hippocampal culture have utilized lentiviral vectors for delivery of ChR2, applied at DIV7 (Boyden et al., 2005; Schoenenberger et al., 2008).

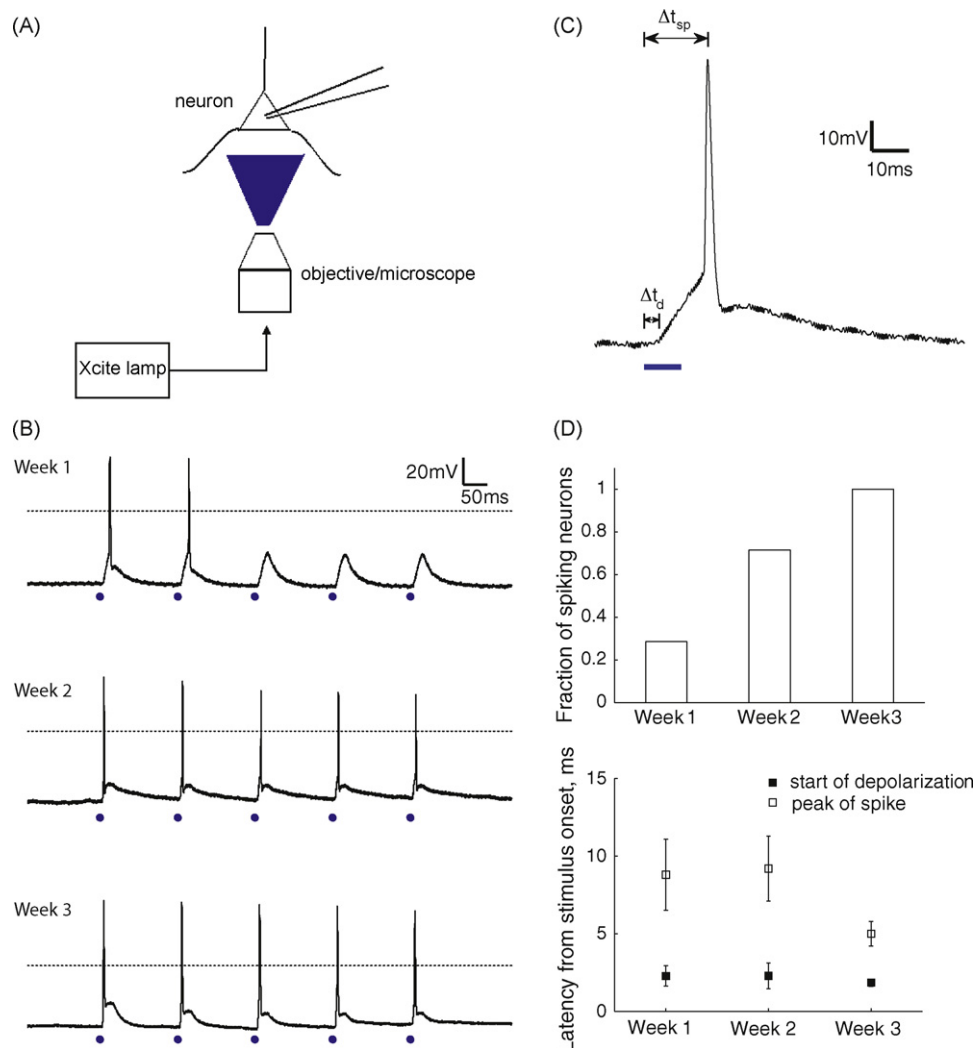


Fig. 2. (A) Schematic of experimental setup showing patched neuron stimulated with widefield illumination. (B) Example recordings from neurons in current clamp from five light stimulations at three different time points in the development of the cultures. The stimulations are indicated with a blue dot and are 10 ms each with frequency 6.25 Hz. Dashed line indicates threshold set at -10 mV, used to determine if neuron fired an action potential or not. (C) Zoomed-in example of an action potential that was stimulated by light. The blue line indicates the 10 ms duration of light stimulation. The latency to depolarization, Δt_d , is the time from the onset of light to the beginning of the photopotential. The latency to the peak of the spike, denoted Δt_{sp} , is the time from the onset of light to the peak of the action potential. These measurements are shown in the bottom panel of D for different time points in development. (D) Upper panel shows the fraction of neurons which spike for every photo stimulus for three different age groups (week 1, $n=7$; week 2, $n=14$; week 3, $n=4$). A neuron was considered to spike if for each of five stimuli (shown in B), the neuron fired an action potential. Lower panel shows the average latencies for photostimulation. Open squares indicate mean latency to depolarization within and across neurons; errorbars indicate standard deviation within and across neurons (week 1, $n=35$ photostimulations; week 2, $n=70$ photostimulations; week 3, $n=20$ photostimulations). Solid squares indicate mean latency to the peak of the action potential for the same age groups. The mean latency was calculated from the average spike latency for individual neurons (week 1, $n=2$ neurons; week 2, $n=11$ neurons; week 3, $n=4$ neurons). Error bars denote the standard deviation for the population of neurons. (For interpretation of the references to color in this figure legend, the reader is referred to the web version of the article.)

100% in week 3 ($n=4$), again consistent with stronger expression levels as observed using fluorescence.

We calculated the mean and standard deviation of the latency from the onset of light to the start of depolarization (Δt_d , see Fig. 2C). As shown in Fig. 2D, for week 1, $\Delta t_d = 2.2 \pm 0.7$ ms ($n=7$ neurons, 5 photostimulations/neuron); for week 2, $\Delta t_d = 2.3 \pm 0.8$ ms ($n=14$ neurons, 5 photostimulations/neuron); and for week 3, $\Delta t_d = 1.8 \pm 0.2$ ms ($n=4$ neurons, 5 photostimulations/neuron). The mean values show that the latencies were about the same for all weeks. The standard deviations are rather small, indicating that the latencies were about the same for all neurons.²

We also calculated the mean and standard deviation of the latency from light onset to the peak of the action potential (Δt_{sp} , see Fig. 2C) for neurons which could be reliably stimulated and averaged the mean and standard deviation for the neurons by week. As shown in Fig. 2D, for week 1, $\Delta t_{sp} = 8.8 \pm 2.3$ ms ($n=2$ neurons); for week 2, $\Delta t_{sp} = 9.2 \pm 2.1$ ms ($n=11$ neurons); and for week 3, $\Delta t_{sp} = 5.0 \pm 0.8$ ms ($n=4$ neurons). Judging from the mean latency, which decreased over time, and the standard deviation, the latency to spiking is more variable than the latency to start of depolarization. This is not surprising, given that the latency to spiking is determined by the time to integrate to threshold, and therefore depends on many factors like the amplitude of the ChR2 current and intrinsic properties of the neuron. Previous measurements found that the latency to spiking was 8.0 ± 1.9 ms for DIV 14 hippocampal culture (Boyden et al., 2005), which is comparable to our measurements.

² Note that all confidence intervals in this paper are standard deviations, rather than standard errors. This is to give some idea of the variability across a population.

3.3. Laser stimulation

The preceding experiments were performed using wide-field stimulation, which lacks the spatial resolution necessary for finding connected pairs of neurons. In our laser stimulation experiments, we chose to focus on the time period between DIV 14 and DIV 21. This is before spontaneous bursting emerges in mass cultures (Pasquale et al., 2008; van Pelt et al., 2004a,b), and our wide-field experiments suggested that it should be possible to stimulate neurons during this time window.

Again we performed current clamp recordings of neurons, this time stimulating them with a laser. Fig. 3B shows an example of a patched neuron, and the blue dot indicates the location of a typical laser stimulation. For these measurements, we targeted the optical stimulation to the soma. The experiments were performed in the presence of CNQX, APV, and bicuculline to ensure that responses were direct rather than synaptically mediated.

Initially, we tuned the laser spot to be approximately 1 μm in diameter. Since the soma of the neurons varied between 10 and 20 μm in diameter, this spot size would keep the stimulation confined to the soma, resulting in high spatial resolution. While depolarization responses were observed, no spikes were stimulated (data not shown). Turning up the intensity caused saturation of the amplitude of the subthreshold depolarization, but still no spikes were observed.

Then we tried 10 and 40 μm spot diameters, indicated by white circles in Fig. 3B, with various intensity values. For both spot diameters we used a 10 ms laser pulse. If a neuron did not spike, increasing the duration beyond this value did not make any difference. This is consistent with previous experiments showing that the photocurrent decays after about 10 ms of photostimulation (Wang et al., 2007).

The threshold luminance for stimulation was about 500 mW/mm^2 .³ Below this value, none of the neurons would fire action potentials when stimulated with the 10 μm spot ($n=4$), and only one response was observed for the 40 μm spot ($n=5$). For luminance values above this threshold, stimulation with the 10 μm spot was reliable for 20% of neurons ($n=5$), and with the 40 μm spot was reliable for 33% ($n=6$) (Fig. 3C, upper panel).

These percentages are lower than for wide-field stimulation. The 40 μm spot illuminated the entire soma and proximal dendrites. Wide-field stimulation also includes more distant sites in the axon and/or dendrites, which could account for its higher success rate.

3.4. Spatial resolution of laser stimulation

We next characterized the spatial resolution of laser stimulation by recording responses in a neuron while illuminating multiple locations arranged in a grid. The grid locations are indicated by the blue circles in Fig. 4A and were spaced approximately 12 μm apart. The locations were stimulated in random order, and the photoresponses were measured. The peak amplitudes of the photoresponses formed a two-dimensional map (Fig. 4B). Again, stimulation was performed in the presence of synaptic blockers.

We estimated the spatial resolution of stimulation by calculating the second moment of distance from the soma, weighted by the amplitude of the map. The square root of this number gave an estimate of the spatial radius of stimulation. The estimation was done separately for subthreshold and spiking responses, and for

each spot size. The standard deviation of the radius was also calculated, to characterize the variability across neurons. For the 10 μm spot, the radius of subthreshold responses was $102.4 \pm 15.4 \mu\text{m}$ ($n=2$), and for the 40 μm spot, the radius of subthreshold responses was $69.5 \pm 2.3 \mu\text{m}$ ($n=3$). Likewise, the radii of superthreshold responses were as follows: 42.2 μm ($n=1$) for the 10 μm spot and $33.7 \pm 11.6 \mu\text{m}$ ($n=2$) for the 40 μm spot. The resolution had little dependence on the size of the laser spot, indicating that the morphology of the neuron could be more important than the spot size in determining the spatial extent of responses. This is perhaps due to activation of ChR2 expressed in the proximal dendrites.

We could probably have obtained better spatial resolution by lowering luminance to the minimum value necessary for producing spikes by somatic illumination, as was shown previously (Schoenenberger et al., 2008). However, it is also important to know the spatial resolution that is possible at luminances above the minimum value.

We might also have obtained better spatial resolution by lowering the spot diameter below 10 μm . However, our experience with the 1 μm spot suggests that better spatial resolution would come only at the cost of drastically reducing the fraction of neurons that can be stimulated reliably.

3.5. Response latencies for laser stimulation

We also measured the latencies from light onset to the peak of the action potentials evoked by laser stimulation targeted to the soma, similar to the measurements reported above for wide-field stimulation. Data were pooled from both 10 and 40 μm laser spots, and various luminances greater than 500 mW/mm^2 . For each of three neurons with action potential responses, we plotted the mean and the standard deviation for the latency to the peak response (Fig. 3C, lower panel). The average of the mean latencies across neurons was $7.8 \pm 2.6 \text{ ms}$ ($n=3$ neurons). The standard deviation of the mean latency across neurons was greater than the standard deviation of the latency for a single neuron.

We also measured the latency to the start of the depolarization, including both super- and subthreshold responses of 11 neurons. For a given spot size, there was little variability between neurons, so all of the data was lumped together. The mean and standard deviation of the latency were $0.9 \pm 0.8 \text{ ms}$ ($n=5$) for the 10 μm spot and $0 \pm 0.4 \text{ ms}$ ($n=6$) for the 40 μm spot.

It is not surprising that the latency to spiking is quite variable across neurons since it depends on the time required for the neuron to integrate the ChR2 current to threshold. The latency to response onset is less variable because it does not include this integration time.

The latencies for laser illumination were similar to those for wide-field stimulation, but slightly less. The latencies for wide-field stimulation are useful for comparison to previous experiments reported in the literature (Boyden et al., 2005). The latencies for laser illumination are more relevant to our attempts to find synaptically connected pairs of neurons, which are reported below.

3.6. A latency criterion for distinguishing between direct vs. synaptic responses

Up to now, we have discussed the case of direct stimulation, intracellular recording in the same neuron that is being subjected to laser illumination. To measure synaptic responses, we must record from a different neuron than the one stimulated by the laser. In an ideal experiment, the neuron chosen for intracellular recording would not express ChR2 at all, so there would be no possibility of direct stimulation. We were not able to find such neurons in our cultures, due to the high rate of AAV infection, so we had to settle for recording from neurons with low but nonzero expression levels.

³ We report luminance value because normalizing by laser spot area calculated from the FWHM provided a clear threshold. Previous results from laser stimulation of single neurons expressing ChR2 were reported for a range of intensity values and spot sizes which were similar to ours (Wang et al., 2007; Schoenenberger et al., 2008).

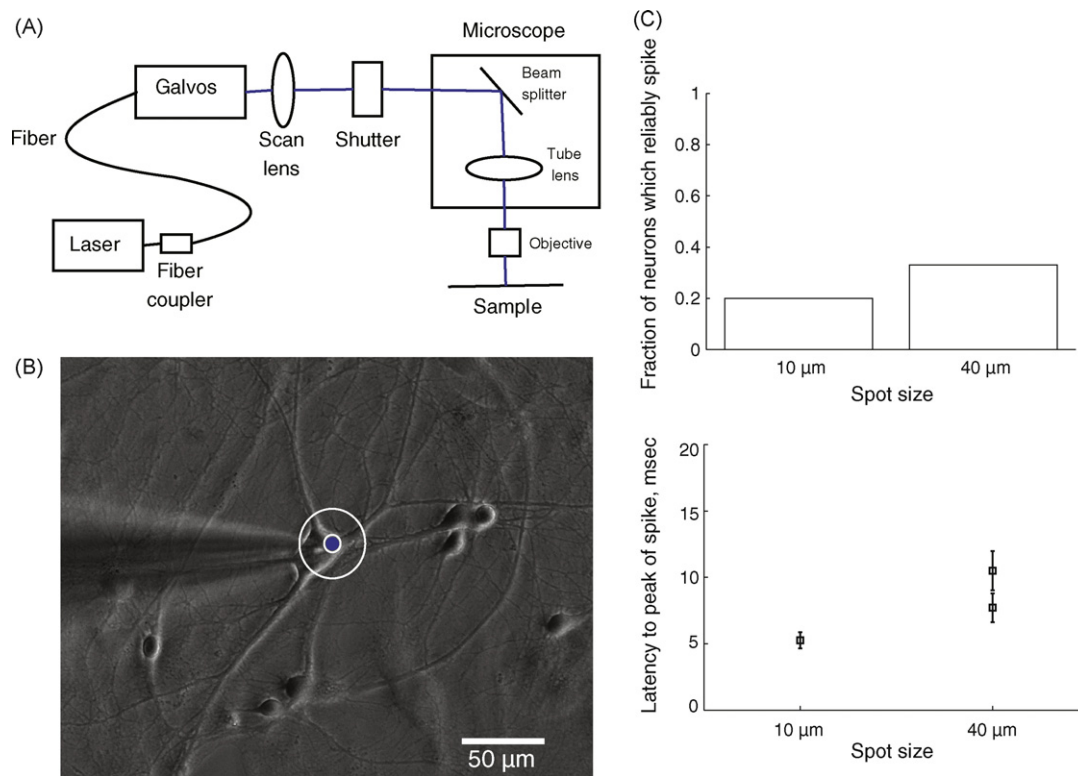


Fig. 3. (A) Optics diagram for laser stimulation. (B) Image of patch clamped neuron at 20 \times magnification. Blue dot indicates the location of the laser stimulation. The concentric white circles show the size of the 10 and 40 μ m diameter spot sizes. (C) Top panel shows the fraction of neurons which spike reliably in response to laser stimulation with luminance greater than 500 mW/mm² for the 10 μ m ($n=5$) and 40 μ m ($n=6$) spot diameters. The lower panel shows the average latencies to the peak of the action potential for three neurons which reliably spiked in response to laser stimulation (measurements from $n=5$ spikes/neuron). The spot diameter is indicated on the x-axis. Error bars denote the standard deviation. (For interpretation of the references to color in this figure legend, the reader is referred to the web version of the article.)

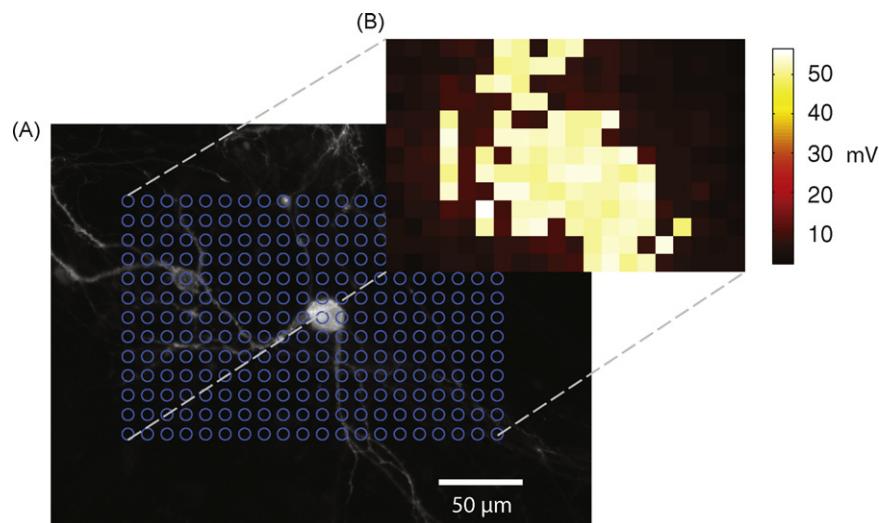


Fig. 4. (A) YFP image of neuron expressing ChR2 at 20 \times magnification. The blue circles indicate the locations of laser stimulation in a grid around the neuron. (B) Colorcoded map of the photoreponse amplitudes in mV, measured from the neuron pictured in panel A. The numerical value of the amplitudes is shown in the colorbar to the right. The spatial locations in the amplitude map correspond to the grid locations in A as indicated by the dashed lines. The white areas in the amplitude map are locations where the laser stimulated action potentials.

As a consequence of this experimental limitation, there was always the possibility of direct stimulation. Because of the low expression levels, the responses to direct stimulation were weak, and hence could be confused with synaptic responses, if amplitude were the only criterion. However, the results of the previous section suggest that latency can be used to distinguish between direct and synaptic responses. We propose that latencies between 0 and 3 ms indicate direct responses, whereas latencies greater than 8 ms

indicate synaptic responses. The latter figure is justified because the latency of a synaptic response should be greater than the latency of spiking in the laser-stimulated neuron, which was measured in the previous section.⁴

⁴ There is substantial variability across neurons in the mean latency to spiking. Furthermore, there is some uncertainty in extrapolating the latency to spiking from

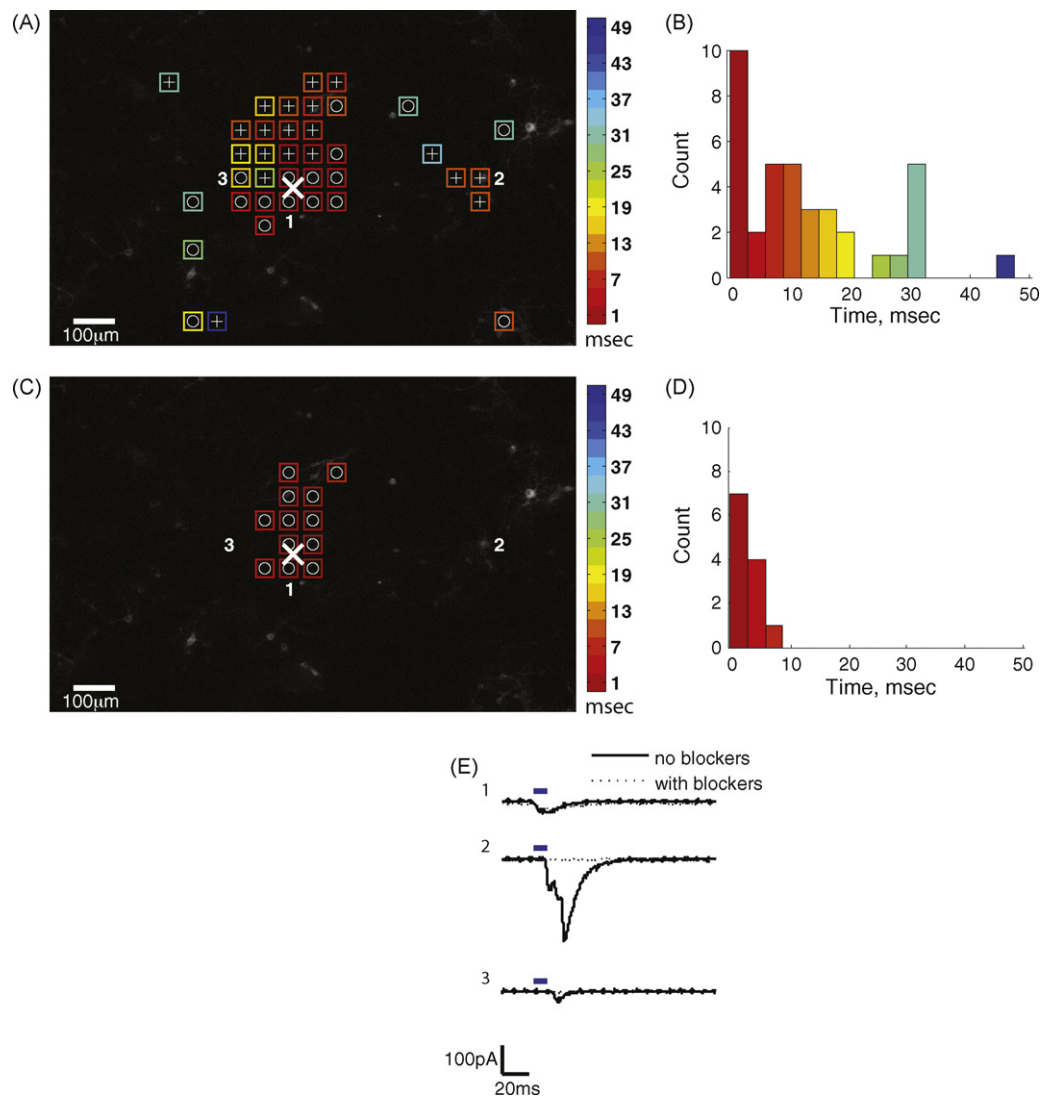


Fig. 5. Image of culture at 4 \times showing YFP fluorescence (A and C). Overlaid is a map of colored squares indicating the latency from onset of light to the start of the photocurrent. The colorbar to the right indicates the magnitude of the latency in milliseconds. The white (X) marks the location of the patch electrode. The (+) markers indicate a complex response, and the (O) markers indicate a simple response in the induced photocurrent. The numbers overlaid in the images in panels A and C correspond to the plots in panel E. They are example traces of currents induced in the recorded neuron for stimulation occurring at the location indicated by the number. Plots 1 and 3 in panel E are examples of simple responses, and plot 2 is an example of a complex response. Panels B and D contain histograms showing the distribution of latencies. The data for A and B were acquired without synaptic blockers. The data for panels C and D were acquired with synaptic blockers.

3.7. Finding synaptic responses by scanning laser stimulation

To test the criterion proposed above, we scanned a 40 μm laser spot across the neural culture while recording from a neuron in voltage clamp which was expressing ChR2 at a very low level, judging from YFP fluorescence. We stimulated locations in a grid in random order using the laser. The experiments were done both with and without synaptic blockers to distinguish between direct and synaptic responses, and the results were compared with the latency criterion. We also used a 4 \times objective for a larger field of view containing more possible laser targets.

For two experiments, Figs. 5 and 6 illustrate the locations in the culture at which laser stimulation produces responses in the voltage clamped neuron, along with a histogram of the observed latencies. Initially, only a subset of locations yielded observable responses in

the voltage clamped neuron (Figs. 5A and 6A), indicating that the laser stimulation has some spatial selectivity. After the addition of synaptic blockers, this subset shrinks (Figs. 5C and 6C). The locations that remain tend to be closer to the cell body of the recorded neuron, consistent with the idea that the synaptic blockers have eliminated the synaptic responses.

To compare with the latency criterion proposed above, the latencies of responses at the various locations are also histogrammed in Figs. 5B and 6B. The addition of synaptic blockers eliminates the responses with latencies greater than 8 ms, and the responses with latencies less than 3 ms are left intact almost completely (Figs. 5D and 6D). Therefore the latency criterion is consistent with the direct and synaptic responses as distinguished pharmacologically.

3.8. Classifying synaptic responses

While it was straightforward to distinguish between direct and synaptic responses, it was more difficult to distinguish between different types of synaptic responses. We were unable to solve

the case of a neuron with an electrode attached to the case of a neuron with no electrode. Nevertheless, it seems improbable that the latency to spiking could drop below 3 ms, the cutoff value we propose as the criterion for a direct response.

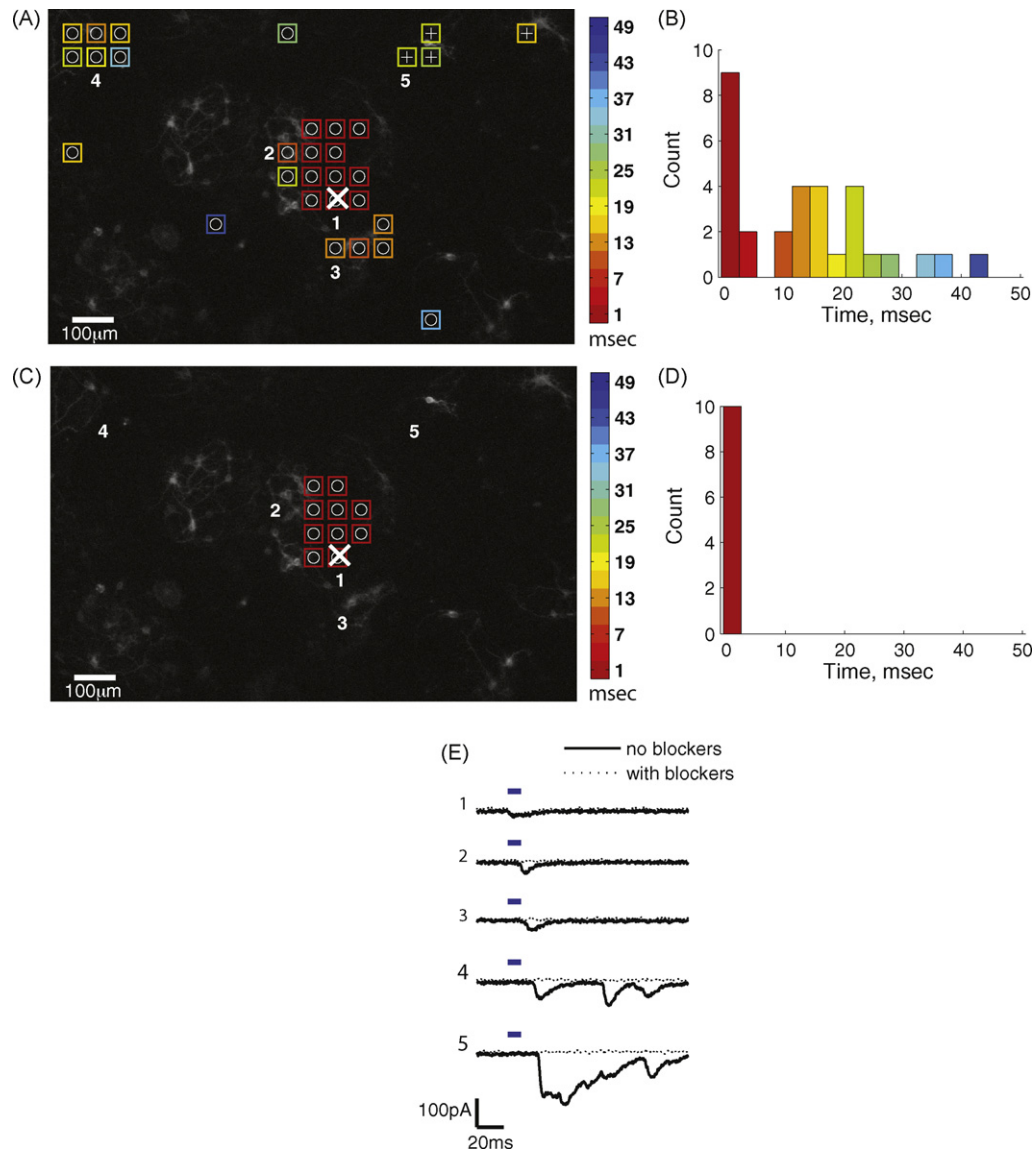


Fig. 6. Another example illustrating the search for synaptic responses. Image of culture at 4 \times showing YFP fluorescence (A and C). Overlaid is a map of colored squares indicating the latency from onset of light to the start of the photocurrent. The colorbar to the right indicates the magnitude of the latency in milliseconds. The white (X) marks the location of the patch electrode. The (+) markers indicate a complex response, and the (o) markers indicate a simple response in the induced photocurrent. The numbers overlaid in the images in panels A and C correspond to the plots in panel E. They are example traces of currents induced in the recorded neuron for stimulation occurring at the location indicated by the number. Plots 1, 2, 3, and 4 in panel E are examples of simple responses, and plot 5 is an example of a complex response. Panels B and D contain histograms showing the distribution of latencies. The data for A and B were acquired without synaptic blockers. The data for panels C and D were acquired with synaptic blockers.

this problem completely, but we can suggest some tentative criteria.

Figs. 5E and 6E show some voltage clamp responses to laser stimulation. Many responses have a simple shape, but sometimes they are quite complex (Fig. 5E, second trace, and Fig. 6E, fourth and fifth traces). Complex responses are presumably the summation of many synaptic pathways, possibly including both monosynaptic and polysynaptic. Complex responses often have large amplitudes, suggesting that laser stimulation has directly or indirectly caused many neurons in the culture to spike.

We suggest that simple responses with small amplitudes and latencies between 8 and 18 ms are candidate monosynaptic responses. Of course, this criterion cannot be entirely reliable, because the latency to spiking of the stimulated neuron shows substantial variability, as discussed earlier. Narrowing the window to a shorter time interval after 8 ms should reduce the number of false positives, but will also reduce the number of true positives.

4. Discussion

We employed rAAV gene delivery to transfer ChR2 to cultured hippocampal neurons. In wide-field stimulation experiments we found that action potentials could be reliably evoked in many neurons after two weeks *in vitro*, as was previously reported for ChR2 delivered via lentivirus (Boyden et al., 2005; Schoenenberger et al., 2008). We further quantified the fraction of neurons that could be reliably stimulated, as a function of weeks *in vitro*.

We then experimented with laser stimulation, which has superior spatial localization compared to wide-field stimulation. These experiments were similar to those of Schoenenberger et al. (2008), except that we focused on the effectiveness of stimulation. We found a decreased fraction of neurons that could be reliably stimulated to generate an action potential through laser illumination of the soma. For example, after two weeks *in vitro*, the fraction of neurons that could be stimulated dropped to 0.35, from 0.8 for

wide-field stimulation. Reducing the laser spot size produced an even smaller fraction of neurons which spike (Fig. 3c). Therefore the reduced effectiveness of laser stimulation is most likely due to smaller photocurrents produced by stimulation of a smaller number of channels.

Finally, we experimented with the use of laser stimulation at locations away from the soma to evoke synaptic responses. These experiments were similar to the wide-field stimulation experiments of Boyden et al. (2005), but with the possibility of obtaining superior spatial resolution. Although we recorded from cells that expressed low levels of ChR2, photostimulation still produced small inward currents even in the presence of synaptic blockers. Based on amplitude alone, these inward currents due to direct stimulation could be confused with synaptic responses observed in the absence of blockers. However, our measurements showed that direct vs. synaptic responses could be distinguished on the basis of response latency (Figs. 5 and 6). We propose that small inward currents that begin less than 3 ms after light onset are the result of direct stimulation.

It is known that synaptic interactions between cultured hippocampal neurons can be very strong, especially in low density cultures, presumably due to multiple synaptic contacts between pairs of neurons (Bekkers and Stevens, 1995; Segal and Furshpan, 1990; Wilcox et al., 1994). The spiking of a single neuron can be sufficient to drive its postsynaptic targets above the threshold for spiking (Segal and Furshpan, 1990). Therefore, complex synaptic responses due to the superposition of many polysynaptic pathways are often observed. This is in contrast to brain slice experiments, in which stimulation of a single neuron causes subthreshold responses in its postsynaptic targets.

Most of our synaptic currents were about 100 pA or less, which is smaller than the currents observed in microisland cultures of the same age. Nevertheless, many synaptic responses to laser illumination were highly complex in their time courses. This could be due to the recruitment of multiple polysynaptic pathways in parallel, and/or stimulation of more than one neuron. Based on our measurements of latency, we suggest that responses with small amplitudes, simple shapes, and latencies between 8 and 18 ms are candidate monosynaptic responses. This criterion cannot be entirely reliable, but it could be a useful guide.

In comparison to other optical methods for stimulating neurons in culture such as glutamate uncaging (Pettit et al., 1997) and optically stimulating neurons grown on silicon wafers (Colicos et al., 2001; Starovoytov et al., 2005), ChR2 fulfills the requirement for reversible, high-speed, spatiotemporal activation of select neuronal populations (Boyden et al., 2005). Repeated trials of single photon photolysis of caged glutamate could release large amounts of glutamate which might lead to toxicity or non-specific stimulation (Callaway and Katz, 1993). Optically stimulating neurons grown on silicon wafers (Colicos et al., 2001; Starovoytov et al., 2005) was another promising method of non-invasive stimulation, but reliably eliciting action potentials meant increasing illumination intensity, which reduced spatial resolution. Additionally, the neurons could only be stimulated to fire action potentials after three weeks *in vitro* (Starovoytov et al., 2005).

Multi-electrode arrays (MEAs) have also been extensively used to probe cultured neural networks (Corner et al., 2002; Pasquale et al., 2008; van Pelt et al., 2004a,b; Wagenaar et al., 2005), namely to characterize the bursting activity in developing cultured neural networks (van Pelt et al., 2004a,b) and control activity in these networks by stimulating at different electrode sites (Madhavan et al., 2006; Massobrio et al., 2007; Wagenaar et al., 2005). However, the extracellular stimulation from the array suffers from poor spatial localization (Heuschkel et al., 2002) and stimulation artifacts (Wagenaar and Potter, 2004). These stimulation issues have been circumvented by using optical stimulation of caged glutamate to

stimulate neurons, while recording extracellular signals via the MEA (Ghezzi et al., 2008). Laser stimulation of neurons expressing ChR2 could potentially be used in a similar fashion, with the advantage that there would be no accumulation of glutamate in the bath.

Acknowledgement

The authors are grateful for support from the Howard Hughes Medical Institute, the Max Planck Society, and the 2008 NSF Emerging Frontiers in Research and Innovation (EFRI) program. We would like to thank Seungeun Oh for assistance with optics, Jeannine Foley for providing hippocampal culture, Rolf Sprengel and Winfried Denk for support.

References

- Arancio O, Kandel ER, Hawkins RD. Activity-dependent long-term enhancement of transmitter release by presynaptic 3',5'-cyclic GMP in cultured hippocampal neurons. *Nature* 1995;376:74–80.
- Arenkiel BR, Peca J, Davison IG, Feliciano C, Deisseroth K, Augustine GJ, et al. In vivo light-induced activation of neural circuitry in transgenic mice expressing channelrhodopsin-2. *Neuron* 2007;54:205–18.
- Atasoy D, Aponte Y, Su HH, Sternson SM. A FLEX switch targets Channelrhodopsin-2 to multiple cell types for imaging and long-range circuit mapping. *J Neurosci* 2008;28:7025–30.
- Auricchio A, Hildinger M, O'Connor E, Gao GP, Wilson JM. Isolation of highly infectious and pure adeno-associated virus type 2 vectors with a single-step gravity-flow column. *Hum Gene Ther* 2001;12:71–6.
- Bekkers JM, Richerson GB, Stevens CF. Origin of variability in quantal size in cultured hippocampal neurons and hippocampal slices. *Proc Natl Acad Sci U S A* 1990;87:5359–62.
- Bekkers JM, Stevens CF. Excitatory and inhibitory autaptic currents in isolated hippocampal neurons maintained in cell culture. *Proc Natl Acad Sci U S A* 1991;88:7834–8.
- Bekkers JM, Stevens CF. Quantal analysis of EPSCs recorded from small numbers of synapses in hippocampal cultures. *J Neurophysiol* 1995;73:1145–56.
- Bi A, Cui J, Ma YP, Olshevskaya E, Pu M, Dzhohor AM, et al. Ectopic expression of a microbial-type rhodopsin restores visual responses in mice with photoreceptor degeneration. *Neuron* 2006;50:23–33.
- Bi GQ, Poo MM. Synaptic modifications in cultured hippocampal neurons: dependence on spike timing, synaptic strength, and postsynaptic cell type. *J Neurosci* 1998;18:10464–72.
- Borrell V, Yoshimura Y, Callaway EM. Targeted gene delivery to telencephalic inhibitory neurons by directional in utero electroporation. *J Neurosci Methods* 2005;143:151–8.
- Boyden ES, Zhang F, Bamberg E, Nagel G, Deisseroth K. Millisecond-timescale, genetically targeted optical control of neural activity. *Nat Neurosci* 2005;8:1263–8.
- Burger C, Gorbatyuk OS, Velardo MJ, Peden CS, Williams P, Zolotukhin S, et al. Recombinant AAV viral vectors pseudotyped with viral capsids from serotypes 1,2, and 5 display differential efficiency and cell tropism after delivery to different regions of the central nervous system. *Mol Ther* 2004;10:302–17.
- Callaway EM, Katz LC. Photostimulation using caged glutamate reveals functional circuitry in living brain slices. *Proc Natl Acad Sci U S A* 1993;90:7661–5.
- Clark AJ, Harold G, Yull FE. Mammalian cDNA and prokaryotic reporter sequences silence adjacent transgenes in transgenic mice. *Nucleic Acids Res* 1997;25:1009–14.
- Colicos MA, Collins BE, Sailor MJ, Goda Y. Remodeling of synaptic actin induced by photoconductive stimulation. *Cell* 2001;107:605–16.
- Corner MA, van Pelt J, Wolters PS, Baker RE, Nuytinck RH. Physiological effects of sustained blockade of excitatory synaptic transmission on spontaneously active developing neuronal networks—an inquiry into the reciprocal linkage between intrinsic biorhythms and neuroplasticity in early ontogeny. *Neurosci Biobehav Rev* 2002;26:127–85.
- Ellis J. Silencing and variegation of gammaretrovirus and lentivirus vectors. *Hum Gene Ther* 2005;16:1241–6.
- Fountain TM, Wood MJ, Wade-Martins R. Delivering RNA interference to the mammalian brain. *Curr Gene Ther* 2005;5:399–410.
- Ghezzi D, Menegon A, Pedrocchi A, Valtorta F, Ferrigno G. A Micro-Electrode Array device coupled to a laser-based system for the local stimulation of neurons by optical release of glutamate. *J Neurosci Methods* 2008;175:70–8.
- Goda Y, Stevens CF. Long-term depression properties in a simple system. *Neuron* 1996;16:103–11.
- Gomperts SN, Carroll R, Malenka RC, Nicoll RA. Distinct roles for ionotropic and metabotropic glutamate receptors in the maturation of excitatory synapses. *J Neurosci* 2000;20:2229–37.
- Gradinaru V, Thompson KR, Zhang F, Mogri M, Kay K, Schneider MB, et al. Targeting and readout strategies for fast optical neural control in vitro and in vivo. *J Neurosci* 2007;27:14231–8.
- Grillner S. Biological pattern generation: the cellular and computational logic of networks in motion. *Neuron* 2006;52:751–66.

- Grimm D, Kay MA, Kleinschmidt JA. Helper virus-free, optically controllable, and two-plasmid-based production of adeno-associated virus vectors of serotypes 1 to 6. *Mol Ther* 2003;7:839–50.
- Hagler Jr DJ, Goda Y. Properties of synchronous and asynchronous release during pulse train depression in cultured hippocampal neurons. *J Neurophysiol* 2001;85:2324–34.
- Hasan MT, Friedrich RW, Euler T, Larkum ME, Giese G, Both M, et al. Functional fluorescent Ca^{2+} indicator proteins in transgenic mice under TET control. *PLoS Biol* 2004;2:e163.
- Hatanaka Y, Hisanaga S, Heizmann CW, Murakami F. Distinct migratory behavior of early- and late-born neurons derived from the cortical ventricular zone. *J Comp Neurol* 2004;479:1–14.
- Heuschkel MO, Fejtli M, Raggenbass M, Bertrand D, Renaud P. A three-dimensional multi-electrode array for multi-site stimulation and recording in acute brain slices. *J Neurosci Methods* 2002;114:135–48.
- Kandel ER. The molecular biology of memory storage: a dialogue between genes and synapses. *Science* 2001;294:1030–8.
- Kaplan MP, Wilcox KS, Dichter MA. Differences in multiple forms of short-term plasticity between excitatory and inhibitory hippocampal neurons in culture. *Synapse* 2003;50:41–52.
- Liewald JF, Brauner M, Stephens GJ, Bouhours M, Schultheis C, Zhen M, et al. Optogenetic analysis of synaptic function. *Nat Methods* 2008;5:895–902.
- Madhavan R, Chao ZC, Wagenaar DA, Bakkum DJ, Potter SM. Multi-site stimulation quiets network-wide spontaneous bursts and enhances functional plasticity in cultured cortical networks. *Conf Proc IEEE Eng Med Biol Soc* 2006;1:1593–6.
- Massobrio P, Baljon PL, Maccione A, Chiappalone M, Martinoia S. Activity modulation elicited by electrical stimulation in networks of dissociated cortical neurons. *Conf Proc IEEE Eng Med Biol Soc* 2007;2007:3008–11.
- Mehrkens JH, Botzel K, Steude U, Zeitler K, Schnitzler A, Sturm V, et al. Long-term efficacy and safety of chronic globus pallidus internus stimulation in different types of primary dystonia. *Stereotact Funct Neurosurg* 2008;87:8–17.
- Miesenbock G, De Angelis DA, Rothman JE. Visualizing secretion and synaptic transmission with pH-sensitive green fluorescent proteins. *Nature* 1998;394:192–5.
- Miyawaki A. Fluorescence imaging of physiological activity in complex systems using GFP-based probes. *Curr Opin Neurobiol* 2003;13:591–6.
- Nagel G, Szellas T, Huhn W, Kateriya S, Adeishvili N, Berthold P, et al. Channelrhodopsin-2, a directly light-gated cation-selective membrane channel. *Proc Natl Acad Sci U S A* 2003;100:13940–5.
- Obeso JA, Rodriguez MC, Gorospe A, Guridi J, Alvarez L, Macias R. Surgical treatment of Parkinson's disease. *Baillieres Clin Neurol* 1997;6:125–45.
- Palmer AE, Tsien RY. Measuring calcium signaling using genetically targetable fluorescent indicators. *Nat Protoc* 2006;1:1057–65.
- Pasquale V, Massobrio P, Bologna LL, Chiappalone M, Martinoia S. Self-organization and neuronal avalanches in networks of dissociated cortical neurons. *Neuroscience* 2008;153:1354–69.
- Petreanu L, Huber D, Sobczyk A, Svoboda K. Channelrhodopsin-2-assisted circuit mapping of long-range callosal projections. *Nat Neurosci* 2007;10:663–8.
- Pettit DL, Wang SS, Gee KR, Augustine GJ. Chemical two-photon uncaging: a novel approach to mapping glutamate receptors. *Neuron* 1997;19:465–71.
- Robertson G, Garrick D, Wilson M, Martin DJ, Whitelaw E. Age-dependent silencing of globin transgenes in the mouse. *Nucleic Acids Res* 1996;24:1465–71.
- Robertson G, Garrick D, Wu W, Kearns M, Martin D, Whitelaw E. Position-dependent variegation of globin transgene expression in mice. *Proc Natl Acad Sci U S A* 1995;92:5371–5.
- Schoenenberger P, Grunditz A, Rose T, Oertner TG. Optimizing the spatial resolution of Channelrhodopsin-2 activation. *Brain Cell Biol* 2008.
- Segal MM, Fushpan EJ. Epileptiform activity in microcultures containing small numbers of hippocampal neurons. *J Neurophysiol* 1990;64:1390–9.
- Shevtsova Z, Malik JM, Michel U, Bahr M, Kugler S. Promoters and serotypes: targeting of adeno-associated virus vectors for gene transfer in the rat central nervous system in vitro and in vivo. *Exp Physiol* 2005;90:53–9.
- Sprengel R, Hasan MT. Tetracycline-controlled genetic switches. *Handb Exp Pharmacol* 2007;178:49–72.
- Starovoytov A, Choi J, Seung HS. Light-directed electrical stimulation of neurons cultured on silicon wafers. *J Neurophysiol* 2005;93:1090–8.
- Sun JY, Chatterjee S, Wong Jr KK. Immunogenic issues concerning recombinant adeno-associated virus vectors for gene therapy. *Curr Gene Ther* 2002;2:485–500.
- Tenenbaum L, Chharto A, Lehtonen E, Velu T, Brotchi J, Levivier M. Recombinant AAV-mediated gene delivery to the central nervous system. *J Gene Med* 2004;6(Suppl. 1):S212–22.
- van Pelt J, Corner MA, Wolters PS, Rutten WL, Ramakers GJ. Long-term stability and developmental changes in spontaneous network burst firing patterns in dissociated rat cerebral cortex cell cultures on multielectrode arrays. *Neurosci Lett* 2004a;361:86–9.
- van Pelt J, Wolters PS, Corner MA, Rutten WL, Ramakers GJ. Long-term characterization of firing dynamics of spontaneous bursts in cultured neural networks. *IEEE Trans Biomed Eng* 2004b;51:2051–62.
- Wagenaar DA, Madhavan R, Pine J, Potter SM. Controlling bursting in cortical cultures with closed-loop multi-electrode stimulation. *J Neurosci* 2005;25:680–8.
- Wagenaar DA, Potter SM. A versatile all-channel stimulator for electrode arrays, with real-time control. *J Neural Eng* 2004;1:39–45.
- Wallace DJ, Borgloh SM, Astori S, Yang Y, Bausen M, Kugler S, et al. Single-spike detection in vitro and in vivo with a genetic Ca^{2+} sensor. *Nat Methods* 2008;5:797–804.
- Wang H, Peca J, Matsuzaki M, Matsuzaki K, Noguchi J, Qiu L, et al. High-speed mapping of synaptic connectivity using photostimulation in Channelrhodopsin-2 transgenic mice. *Proc Natl Acad Sci U S A* 2007;104:8143–8.
- Wilcox KS, Buchhalter J, Dichter MA. Properties of inhibitory and excitatory synapses between hippocampal neurons in very low density cultures. *Synapse* 1994;18:128–51.
- Xia X, Zhang Y, Ziehl CR, Zhang SC. Transgenes delivered by lentiviral vector are suppressed in human embryonic stem cells in a promoter-dependent manner. *Stem Cells Dev* 2007;16:167–76.
- Zhang YP, Holbro N, Oertner TG. Optical induction of plasticity at single synapses reveals input-specific accumulation of alphaCaMKII. *Proc Natl Acad Sci U S A* 2008;105:12039–44.
- Zhang YP, Oertner TG. Optical induction of synaptic plasticity using a light-sensitive channel. *Nat Methods* 2007;4:139–41.
- Zhu P, Aller MI, Baron U, Cambridge S, Bausen M, Herb J, et al. Silencing and un-silencing of tetracycline-controlled genes in neurons. *PLoS ONE* 2007;2:e533.